Available online at www.sciencedirect.com
ScienceDirect
ELSEVIER
Wear xxx (2007) xxx–xxx
WEAR
www.elsevier.com/locate/wear

An in situ mechanism for self-replenishing powder transfer films: Experiments and modeling

C.F. Higgs III*, E.Y.A. Wornyoh

Carnegie Mellon University, Mechanical Engineering Department, Pittsburgh, PA 15217-3890, USA

Received 9 August 2006; received in revised form 9 March 2007; accepted 26 March 2007

Abstract

Pellets were formed by compacting MoS_2 powder. A series of tests were conducted on a tribometer that consisted of simultaneous pellet-on disk and pad-on disk sliding contacts. The purpose of the tests was to intentionally transfer MoS_2 third-body particles to a disk where its lubrication characteristics could be studied. This work also showed that the MoS_2 pellet actually acted as a self-repairing, self-replenishing, oil-free lubrication mechanism. In the experiment, a pellet is sheared against the disk surface while the loaded slider rides on the lubricated surface and depletes the deposited powder film. A control-volume fractional coverage modeling approach was employed to predict both (1) the friction coefficient at the pad/disk interface and (2) the wear factor for the lubricated pellet/disk sliding contact. The fractional coverage varies with time and is a useful modeling parameter for quantifying the amount of third body film covering the disk asperities. In the model, the wear rate of a pellet and pad friction coefficient can be determined as a function of the pellet load, slider pad load, disk speed, and material properties. Results from the model qualitatively and quantitatively predict the tribological behavior of the experimental sliding contacts reasonably well.

Keywords: Powder lubrication; In situ solid lubrication; Transfer film; Fractional coverage; Particulate lubrication

1. Introduction to powder lubrication

Advancements in engine technologies and the continuing depletion of the world's petroleum oil supply have increased the need for oil-free lubrication. Additionally, conventional liquid lubricants have proven inadequate in extreme-temperature and load environments. Fortunately, lamellar powders or "powder lubricants" such as molybdenum disulfide (MoS_2), titanium dioxide (TiO_2) and tungsten disulphide (WS_2) have demonstrated excellent tribological capabilities [1]. In powder lubrication, powders lubricate by forming transfer films from compact, spray, or composite forms. In this paper, the lubricant source is obtained from powder compacts intentionally sheared against a rotating disk surface. Consequently, a thin transfer film is formed on the surface on the order of the surface roughness. Therefore, thick film powder lubrication theory, such as Heshmat's quasi-hydrodynamic theory, does not apply to these thin asperity-covering transfer films.

1.1. Compacted powder transfer films

Powder lubricants, pelletized to serve as a deposition source, present a novel approach to lubricating machine components in future applications. Research has shown that pellets can be successfully applied as transfer films to tribosurfaces [2–4]. Additionally, Haltner compacted powder lubricants as a mechanism for transferring a thin lubricious film to a rotating disk [5]. He studied MoS_2 compacts in both vacuum and in room air (relative humidity of 50%), at a velocity of 0.84 m/s. In these tests, the steady-state friction coefficient was $\mu = 0.17$. Compacted MoS_2 powders have also exhibited transient frictional behavior in tests done under both non-vacuum [1] and vacuum [6] conditions. Johnson and Vaughn, who did their tests in vacuum, concluded that the "buildup" in initial friction values was due to an amorphous layer of sulfur generated at the initial point of sliding. Higgs and Heshmat, who conducted tests under non-vacuum (i.e., atmospheric conditions at room temperature) introduced an alternate explanation to the build-up friction relating it to disorder as quantified by entropy [1]. The traction behavior of powder graphite compacted at Hertzian pressure levels was studied to characterize the behavior of the powder particles in the contact

* Corresponding author. Tel.: +1 412 268 2486; fax: +1 412 268 3348.
E-mail address: higgs@andrew.cmu.edu (C.F. Higgs III).

0043-1648/$ – see front matter © 2007 Published by Elsevier B.V.
doi:10.1016/j.wear.2007.03.026

region [7]. In the disk-on-disk tribometer used in their experiments, the speed was $U = 3.98$ m/s (100 rpm) and the Hertzian pressure $P_c = 690$ MPa. From their work, a method was developed for predicting the film thickness of a powder film in a Hertzian contact, and the traction coefficient of a powder film in rolling element bearing configurations. Higgs et al. showed that MoS_2 pelletized powder lubricants acted as a velocity accommodating third-body in high-speed sliding contacts [1]. Extending Godet's third-body approach [8], Fillot et al. [9] used a computational wear simulation to glean mass balance laws for describing wear between tribosurfaces when a third-body is formed.

The scope of this work presents experimental results from a competing transfer film deposition and lubricant depletion process. To predict this process, a control volume fractional coverage (CVFC) model has been developed that extends the mass-balance concepts of Fillot et al. [9] to analyze the competing pellet transfer film (i.e., lubricant deposition) and pad wear (i.e., lubricant depletion) mechanisms on a pellet-on disk with slider pad tribometer configuration. Results from the pellet-on-disk with slider experiments are compared to the theoretical results from the CVFC model.

2. Experimental details

2.1. Pellet-on disk experiments

To analyze an in situ powder transfer film mechanism, a setup consisting of in-line sliding of a MoS_2 pellet and slider pad (Fig. 1) was developed. Pellets fabricated from tap powder are wear tested on the pellet-on-disk tribometer (Fig. 2), using the in-line pellet and slider setup of Fig. 1. In the wear tests, MoS_2 pellets were sheared against the surface of the rigid rotating disk. The thin-film interfacial third body particulates produced by the pellet were depleted by the loaded slider pad riding on the lubricated surface.

2.2. Fabricating pellets for wear testing

Preliminary work identified MoS_2 powder as a suitable solid lubricant material for this investigation [2]. A powder compaction system was designed for forming the cylindrical MoS_2 pellets, consisting of a top and bottom die, which housed the

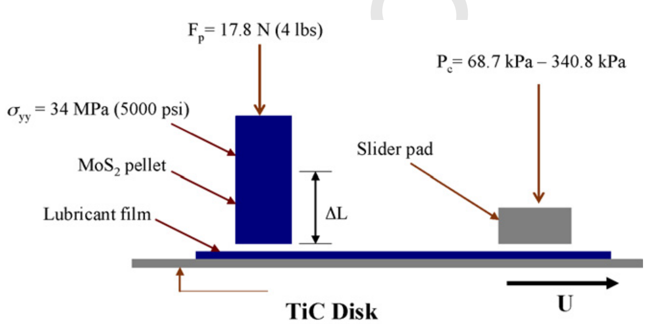

Fig. 1. Pellet-on-disk with slider apparatus enables the study of self-replenishing powder film transfer. The test parameters were as follows: $F_p = 17.8$ N; $P_c = 68.7$–340.8 kPa; $U = 4.5$–45 m/s.

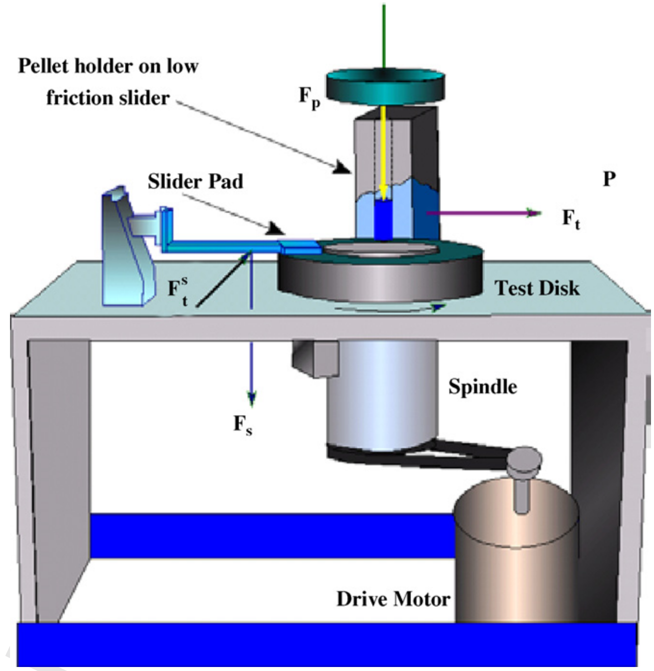

Fig. 2. Pellet-on-disk with slider tribometer for measuring the pellet wear and friction forces at pellet/disk and slider/disk.

powders during compaction. A thin sleeve of Inconel alloy encompassed the powders. A porous, split sleeve tube encasing the powder and the Inconel was placed in the bore of the top die. This encasing was rested on top of a porous disk located at the base of the bore. The disk had a porosity of 0.5 μm and allowed the air in the powders to escape during compaction. The piston was less than 100 μm smaller than the porous encasing to avoid metal-to-metal contact. Once filled with powder, the fixture was placed under a hydraulic press where it was compacted to the desired pressure. The resulting pellet had a diameter of 19 mm and a length of 51 mm. The pellets were made by compacting three different samples of MoS_2 powder with varying average particle sizes; Sample A with 13.64 μm; Sample B with 7.4 μm; Sample C with 1.56 μm. Similar to transfer films that are not self-replenishing [10], Sample A was used in previous pellet-on-disk tests conducted without slider pads and was excluded as a self-replenishing solid lubricant candidate for this work, so only Samples B and C are examined in this study. The mass, diameter, length, and density of the pellet were measured after compaction.

2.3. Pellet-on disk with slider experiments

After the pellets were fabricated and measured, they were placed in the L-shaped pellet holder for wear testing. During the tests, a pellet was loaded against the disk, as it rotates. A slider pad, located in-line with the pellet, was also loaded against the disk. In this project, the investigation of the film transfer process was studied using the pellet-on-disk wear test. Fig. 1 shows a diagram of the pellet-on-disk with slider pad configuration. In the experiment, a powder transfer film from a pellet was deposited on the disk and a slider pad depletes the film when its load exceeds the film's load carrying capacity. Since the pellet is pressed against the rotating disk by a weight F_p, the thin film is transferred to the disk by shearing. The transfer film supports the normal load on the slider, which is expressed as a contact pressure P_c. Lastly, the wear rate (i.e., transfer film delivery rate) of the pellet and the frictional behavior at the pellet-disk and pad/disk interfaces were studied.

2.4. Experimental setup

A schematic of the tribometer is shown in Fig. 2. The tribometer from Mohawk Innovative Technology Inc. [1], consisted of a disk mounted on a spindle driven by a one HP variable-speed DC motor, which had a maximum speed of approximately 5000 rpm. The disk, made of Titanium Carbide cermet (TiC), had an average test track radius of 83.1 mm (3.27 in.) and a thickness of 14 mm. A pellet lubricant holder for the test specimen maintained the pellet in a vertical position. The holder, mounted atop a low friction slider, allowed the pellet to slide without constraint against the rotating disk. A load cell with a probe wire attached to the base of the specimen holder measured the frictional force exerted on the pellet. A linear variable differential transformer (LVDT) with a resolution of 2.5 μm was placed on top of the pellet to record its vertical displacement, which was converted to the mass of material worn vertically. This calculated vertical mass wear was verified against the total mass of wear measured at the completion of the tests using a mass balance.

The measurables in the experiments are shown in Fig. 2 as the frictional (tangential) force F_t^S at the slider pad, the frictional force at the pellet F_t^P, and the wear displacement of the pellet AL (see Fig. 1).

The high-speed pellet-on-disk tribometer was modified to include a load arm capable of securing a slider pad on the disk during wear tests. The slider pad supports the load on the film and was loaded by placing dead weights F_s on the load arm at a distance away from the pad's center of mass. Since the point load was not being applied at the pad, a moment balance was made to determine the load actually realized at the pad, which was transmitted by a pivot ball. At the pivot ball on the load arm, the contact pressure P_c on the bearing pad was computed by dividing the normal load F_s by the pad area and multiplying this quotient by a moment factor. This factor, 0.719, was determined by taking the summation of moments about the load arm joint and was used to determine the load actually experienced at the center of the pad. The contact area of the pad was 6.45 cm^2 (1 in.^{2}) and a photograph of the slider pads are shown in Fig. 3.

A graphical user interface data acquisition software was developed and used to record the relevant parameters of speed, friction forces, and pellet vertical displacement at acquisition time intervals as small as a tenth of a second. Digital panel meters also displayed the output values for manual verification, and an alarm was designed to warn the user when the dry friction coefficient was attained between the slider and disk.

2.5. Pellet-on disk with slider testing procedure

Testing was initiated when the disk reached the prescribed speed. The data acquisition is started at the same time. To ensure reliability, data is also acquired manually by reading the digital panel meters, measuring the average wear depth and friction forces. A special receptacle collects the wear debris emerging from the interface. At the end of each run, the structural integrity of the pellet is visually examined, and the disk cleaned using hexane for the next run. The amount of wear for a particular run is experimentally determined by computing the product of the pellet cross sectional area, pellet density, and vertical displacement (i.e., change in pellet length) as measured by the LVDT system. The mass wear of the pellet is also obtained using a mass balance with a resolution of 0.05 g. The LVDT-based wear from experiments is compared to the mass balance wear at the conclusion of the tests. The LVDT computed pellet mass loss was within 5% of the mass loss in wear tests. The in situ measurements were vertical pellet wear ΔL and the pad and pellet coefficient of friction are μ_s and μ_p, respectively. Numerous pellet-on-disk with slider tests were conducted under normal room conditions with the following experimental parameters shown in Table 1.

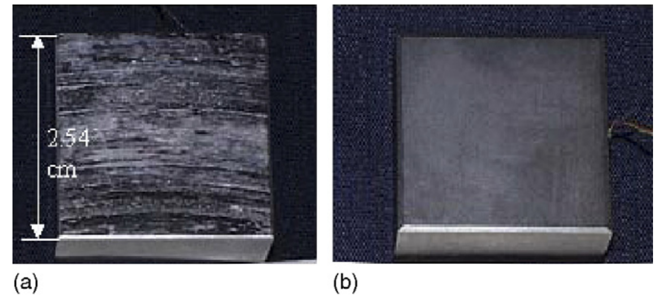

Fig. 3. Photographs of TiC slider pads: (a) pad was wear tested for 180 km and (b) pad was untested pad.

3. Experimental results

The wear tests consist of a pellet-on-disk with a slider pad depleting the film track deposited by the pellet. The series of wear tests show wear and friction trends of the pellet and pad as a function of distance. The results depict the behavior of the pellet as a function of disk speed U, load on pellet F_p, powder compaction pressure σ_{yy}, and pad load, F_s. Friction coefficients at the pellet/disk interface μ_p and slider/disk interface μ_p were also measured (from the frictional forces) to assess the frictional behavior of the powder film at the two sliding contact regions. The vertical wear ΔL of the pellet was also measured

Table 1
Experimental parameters for pellet-on disk tests

Parameter	Value
Ambient temperature (°C)	23.3–24.4
Relative humidity (%)	40–50
Test speed, U (m/s)	4.5–45
Compaction pressure, σ_{yy} (MPa)	34.5
Pellet load, F_p (N)	17.8
Pad load, F_s (N)	56.8–307
Range of test sliding distance (km)	6–8
Average MoS_2 powder particle sizes	Samples B (7.4 μm) and C (1.56 μm)

Please cite this article in press as: C.F. Higgs III, E.Y.A. Wornyoh, An in situ mechanism for self-replenishing powder transfer films: Experiments and modeling, Wear (2007), doi:10.1016/j.wear.2007.03.026

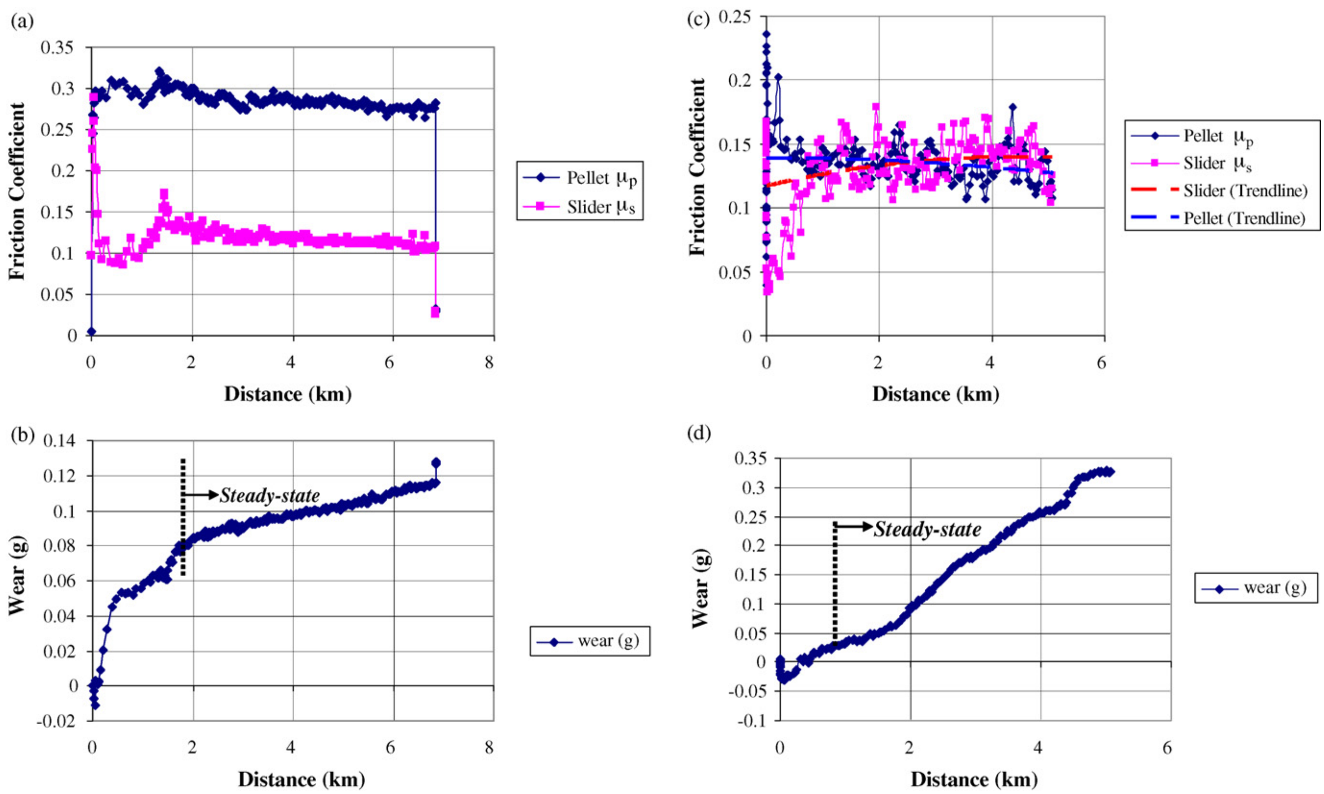

Fig. 4. Data from a single pellet-on-disk with slider test for pelletized MoS_2 on a TiC disk. (a and c) Pellet and pad friction coefficient; (b and d) cumulative pellet wear. (a and b) Test (#55) conditions for Sample B (σ_{yy} = 34.5 MPa), P_c = 137.8 kPa (20 psi), U = 9 m/s; (c and d) Test (#80) conditions for Sample C (σ_{yy} = 34.5 MPa), P_c = 340.14 kPa (49.6 psi), U = 27 m/s.

and converted into mass wear loss. While there were numerous tests conducted on the tribometer, the authors exercise brevity by showing data friction and wear at one test condition in Fig. 4. Summary data are shown for both Samples B and C pellets at two additional disk speeds U = 27 m/s and 45 m/s in Figs. 5 and 6, respectively. The friction and wear data at these speeds show trends that are representative of the other pellet-on disk with slider tests.

Fig. 4(a) and (b) shows data from a wear test with the MoS_2 pellet Sample B (P_d = 7.4 μm) at a compaction pressure σ_{yy} = 34.5 MPa, slider pad contact pressure P_c = 137.8 kPa, and disk speed U = 9 m/s. In Fig. 4a, the pellet friction coefficient μ_p is shown as a function of wear distance L_T. The friction coefficient was determined by the quotient of the frictional force F_t^P measured at the base of the pellet and the normal load produced on the disk by the pellet (see Fig. 2). It is not evident from the μ_p versus distance graphs what the tribological effect on the pads would be. However, it seems that μ_p may be useful in estimating the tangential force needed to detach the MoS_2 particles from the pellet [11]. Detachment forces, which relate to pellet wear, may be discernable by looking at the μ_p plot. In Fig. 4a, the slider friction coefficient μ_s is shown as a function of distance. The friction coefficient μ_s was determined by the quotient of the frictional force F_t^S measured at the base of the slider pad and the normal load produced on the disk by the pad. During run-in, the slider friction coefficient μ_s decreased below the dry friction coefficient ($\mu_s = 0.2$) until it reached the lowest friction coefficient for the test of $\mu_s = 0.08$. Steady-state conditions (i.e., when the wear rate becomes constant) for the test were reached at approximately 2 km at which point $\mu_s = 0.13$. This shows that the pad did not experience starvation during the 5 km at steady state. Fig. 4b shows the mass loss of pel-

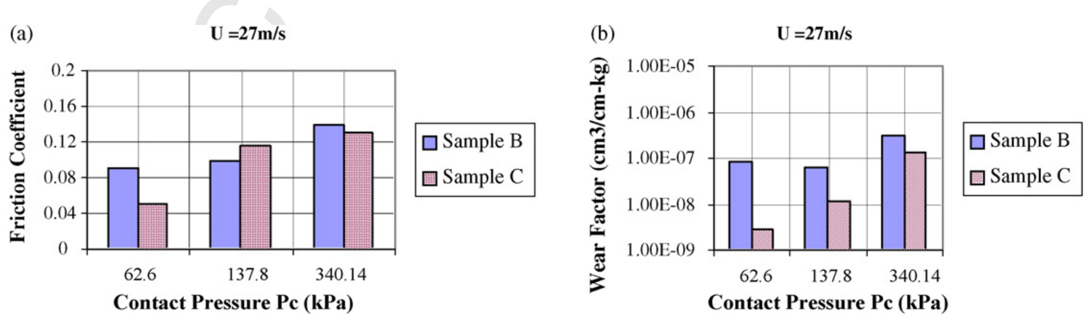

Fig. 5. (a) Slider pad friction and (b) pellet wear as a function of slider contact pressure. Test conditions: U = 27 m/s, σ_{yy} = 34.5 MPa, F_p = 21.3 N.

Please cite this article in press as: C.F. Higgs III, E.Y.A. Wornyoh, An in situ mechanism for self-replenishing powder transfer films: Experiments and modeling, Wear (2007), doi:10.1016/j.wear.2007.03.026

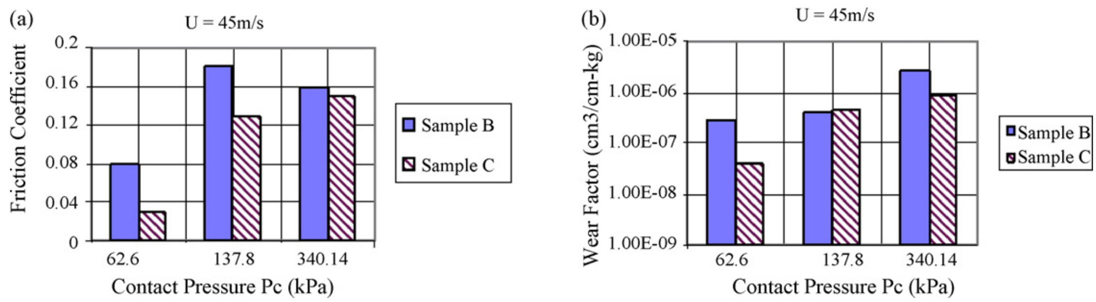

Fig. 6. (a) Slider pad friction and (b) pellet wear as a function of slider contact pressure. Test conditions: $U = 45$ m/s, $\sigma_{yy} = 34.5$ MPa, $F_p = 21.3$ N.

let wear as a function of distance L_T. The corresponding wear factor ϕ, which is the *steady state* wear volume divided by the product of the mass-load on the pellet and the total wear distance, is $1.07 \times 10^{-8}\ \mathrm{cm^3\ cm^{-1}\ kg^{-1}}$. The ϕ was approximately constant for 5 km indicating that there was a continuous delivery of powder lubricant being supplied to the pad/disk sliding contact. In another test, Fig. 4(c) and (d) shows data with the MoS_2 pellet Sample C ($P_d = 1.56$ μm) at a compaction pressure $\sigma_{yy} = 34.5$ MPa, slider pad contact pressure $P_c = 340.14$ kPa, and disk speed $U = 27$ m/s. In Fig. 4c, one can see that both the pad and pellet friction coefficients approach steady-state values in the approximate range of 0.13–0.15. This corresponds to a steady-state wear rate which starts at approximately a wear distance of 1 km as shown in Fig. 4d.

The results from the pellet-on disk with slider wear tests for both MoS_2 powder Samples B and C have been summarized using the bar charts in Figs. 5 and 6 which represent wear tests at $U = 27$ m/s and 45 m/s, respectively. The normal load on the pad creates a contact pressure P_c (in kPa) on the disk. In Figs. 5 and 6, the steady-state friction coefficient μ_s at the slider/disk interface and the wear factor ϕ as a function of P_c are shown. At $U = 27$ m/s, Fig. 5a shows that the friction coefficient increases with the pad load for both samples. In Fig. 5b, the wear factor also increases with increasing slider load, except for Sample B at $P_c = 137.8$ kPa. At $U = 45$ m/s, Fig. 6a shows that the friction coefficient at the pad/disk interface increases with contact pressure. However, Sample B slightly deviates from the global trend at $P_c = 137.8$ kPa. In Figs. 5 and 6, Sample C consistently shows that the pad friction coefficient and pellet wear rate ϕ both increase with pad load. This likely suggests that increasing the pad load increased the lubricant starvation which made the friction coefficient also increase. Consequently, the pellet wear rate increased as the disk starvation (i.e., lubricant-depletion) promoted increased pellet wear. In Fig. 6b, the pellet's wear increases as the load on the pad increases for both MoS_2 samples. It is likely that environmental fluctuations such as humidity may have caused the slight deviations from the expected trends for Sample B in Figs. 5b and 6a. In Figs. 5b and 6b, one can see that the pellet with Sample C powder wears less than Sample B pellet for almost all contact pressures. This is attributed to the fact that for a prescribed compaction pressure, Sample C powder (i.e., the smaller particles) was more dense with higher cohesion. Another telling feature of Figs. 5b and 6b is that a larger pad load increased pellet wear. As the film was depleted, the wear rate of the pellet increased to account for the lack of lubricant film present on the disk. This suggests the lubrication mechanism appears to replenish the transfer film only as-needed. One should note that Fig. 4c and b is the friction and wear evolution data for the test which is summarized in Fig. 5 ($U = 27$ m/s; Sample C) when $P_c = 340.14$ kPa.

4. Theory

Fig. 7 shows a simplified schematic of the pellet as it is sheared against the disk whose surface asperities have been exaggerated. The third body particulates sheared from the pellet fill up the valleys on the disk surface en route to covering up the asperities.

4.1. The control volume fractional coverage (CVFC) model

In order to develop a first principle tribology model of the lubrication process, the third-body transfer film was made the control volume. Next, a wear and third body concept was adopted [9]. As the pellet in Fig. 7 wears, it deposits a thin film of lubricant on the surface of the disk and covers the asperities on the disk surface. The control volume fractional coverage (CVFC) modeling assumptions are as follows:

(i) The slider/disk and pellet/disk interface topographies are represented by a nominally flat pellet or slider surface in contact with a rough disk with a composite roughness.
(ii) The disk topography varies little relative to the maximum asperity height h_{max}.
(iii) The frictional response in the pellet/disk and slider/disk interfaces is predominantly a function of the amount (i.e., fraction) of transfer film covering the disk surface.

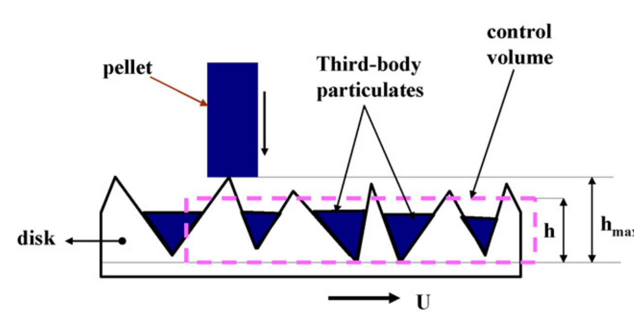

Fig. 7. Schematic of pellet sheared against the disk.

Please cite this article in press as: C.F. Higgs III, E.Y.A. Wornyoh, An in situ mechanism for self-replenishing powder transfer films: Experiments and modeling, Wear (2007), doi:10.1016/j.wear.2007.03.026

The fractional coverage, X, is dimensionless and is defined as the fraction of lubricant (third body particulates) that covers the asperities of the disk surface. That is:

$$X = \frac{h}{h_{\max}} \tag{1}$$

where h is the local height of third body film. The film height when the disk asperities are completely covered is $h = h_{\max}$ and in that case, $X = 1$. Similarly, $X = 0$ represents the case of no lubricant coverage. Researchers have employed other forms of fractional coverage relations in modeling lubrication processes [12–17]. Our model assumes that the slider pad can be treated as smooth and that the frictional response is primarily a function of the change in the film height h of solid lubricant that covers the asperities. Referring to Fig. 7, consider the control volume that encloses asperities and valleys as well as the third body particulates transferred by the pellet as shown by the dotted lines. The third body has the pellet as its sources of supply, however, it is being depleted from two sources: at the pellet's leading edge, and far away from the pellet, at the slider. From conservation of mass:

$$\begin{pmatrix}\text{Third Body}\\ \text{Storage Rate}\end{pmatrix} = \begin{pmatrix}\text{Third Body}\\ \text{Input Rate}\end{pmatrix} - \begin{pmatrix}\text{Third Body}\\ \text{Output Rate}\end{pmatrix} \tag{2}$$

To mathematically interpret Eq. (2), use is made of Archard's Wear Law:

$$\dot{V} = K F_{\mathrm{N}} U \tag{3}$$

where $\dot{V}$ is the volume wear rate, K the dimensional wear coefficient, F_{N} the normal load applied, and U is the sliding velocity. K is an empirical constant that usually describes the probability of wear occurring between two different materials such as TiC on MoS_2, although in some instances, K could just be between the same kind of material for instance MoS_2 pellet riding on MoS_2 third body. Using Archard's wear law from Eq. (3), the conservation law of Eq. (2) becomes:

$$A\frac{\mathrm{d}h}{\mathrm{d}t} = K_{\mathrm{p}} F_{\mathrm{p}} U \left(1 - \frac{h}{h_{\max}}\right) - K_{\mathrm{ep}} F_{\mathrm{p}} U \frac{h}{h_{\max}} - K_{\mathrm{es}} F_{\mathrm{s}} U \frac{h}{h_{\max}} \tag{4}$$

where A is the cross-sectional area, and F_{p} and F_{s} are pellet and slider loads, respectively. Additionally, K_{p} is the wear coefficient for the pellet/disk interface, while the wear coefficients for the third body wear due to shearing from the pellet and slider pad are K_{ep} and K_{es}, respectively. Applying the definition of fractional coverage from Eqs. (1)–(4) yields:

$$A h_{\max}\frac{\mathrm{d}X}{\mathrm{d}t} = K_{\mathrm{p}} F_{\mathrm{p}} U (1 - X) - K_{\mathrm{ep}} F_{\mathrm{p}} U X - K_{\mathrm{es}} F_{\mathrm{s}} U X \tag{5}$$

Eq. (5) is the governing equation which together with the initial condition $X(0) = 0$ completely defines the problem for the CVFC model. The solution to Eq. (5) is given by:

$$X(t) = \frac{F_{\mathrm{p}} K_{\mathrm{p}}}{F_{\mathrm{s}} K_{\mathrm{es}} + F_{\mathrm{p}}(K_{\mathrm{ep}} + K_{\mathrm{p}})}\left[1 - \exp\left(-\frac{t}{\tau}\right)\right] \tag{6}$$

where t is the time constant defined by:

$$\tau = \frac{A h_{\max}}{F_{\mathrm{s}} K_{\mathrm{es}} + F_{\mathrm{p}}(K_{\mathrm{ep}} + K_{\mathrm{p}}) U} \tag{7}$$

After a long time has elapsed, the steady state fractional coverage is deduced from Eq. (6) as:

$$X_{\mathrm{ss}} = \frac{F_{\mathrm{p}} K_{\mathrm{p}}}{F_{\mathrm{s}} K_{\mathrm{es}} + F_{\mathrm{p}}(K_{\mathrm{ep}} + K_{\mathrm{p}})} \tag{8}$$

Researchers have used other forms of fractional coverage to predict the friction coefficient. Adopting the linear-rule-of-mixtures from Dickrell et al. [18,19], the pellet and slider friction coefficients can be defined as:

$$\mu_{\mathrm{p}} = X\mu_{\mathrm{lub,p}} + (1 - X)\mu_{\mathrm{dry,p}} \tag{9}$$

$$\mu_{\mathrm{s}} = X\mu_{\mathrm{lub,s}} + (1 - X)\mu_{\mathrm{dry,s}} \tag{10}$$

where μ_{p} and μ_{s} are friction coefficients at the pellet/disk and slider/disk interfaces, respectively. The pellet and slider friction coefficients for unlubricated conditions are $\mu_{\mathrm{dry,p}}$ and $\mu_{\mathrm{dry,s}}$ while those for lubricated conditions are indicated by $\mu_{\mathrm{lub,p}}$ and $\mu_{\mathrm{lub,s}}$.

To obtain the steady-state wear factor of the pellet, ϕ, Eq. (5) is first rewritten for the pellet alone:

$$\dot{V}_{\mathrm{p}} = \frac{\mathrm{d}V_{\mathrm{p}}}{\mathrm{d}t} = K_{\mathrm{p}} F_{\mathrm{p}} U (1 - X(t)) \tag{11}$$

Thus,

$$V_{\mathrm{p,total}} = \int_0^{t_{\mathrm{s}}} K_{\mathrm{p}} F_{\mathrm{p}} U (1 - X(t))\,\mathrm{d}t \tag{12}$$

where V_{p} is the pellet wear volume, $V_{\mathrm{p,total}}$ is the total pellet wear volume over a total sliding time t_{s}. Then, the result from Eq. (12) is used in Archard's wear law to give the steady-state wear factor as:

$$\phi\,(\mathrm{cm^3\,cm^{-1}\,kg^{-1}}) = \frac{V_{\mathrm{p,total}}}{(F_{\mathrm{p}}/g) t_{\mathrm{s}} U} \tag{13}$$

where g is gravitational acceleration.

Table 2 has the numerical values that were used in the CVFC model. Based on Eq. (5), the wear coefficients K_{p} and K_{es} represent the probability of the MoS_2 *pellet* being worn by the TiC disk and the probability that the MoS_2 film will be removed from the disk by the trailing TiC *slider* pad, respectively. Thus, both of these sliding contacts involve a TiC-on-MoS_2 interface configuration (Fig. 2), and it was assumed that $K_{\mathrm{p}} \cong K_{\mathrm{es}} = 5.5 \times 10^{-8}\ \mathrm{m^2/N}$, as shown in Table 2. The final wear coefficient K_{ep} represents the lower probability that the MoS_2 pellet will become glazed and thus removes MoS_2 transfer film from the disk. Since this event happened less frequently in the tests, we assigned this wear coefficient with an order of magnitude lower probability of $K_{\mathrm{ep}} = 5.5 \times 10^{-9}\ \mathrm{m^2/N}$. These values represent our best guess and can be improved through detailed curve fitting. The authors chose not to curve-fit here to demonstrate the reasonable effectiveness of the first-principle CVFC model. The other values in Table 2 were taken to coincide with the experimental conditions.

Please cite this article in press as: C.F. Higgs III, E.Y.A. Wornyoh, An in situ mechanism for self-replenishing powder transfer films: Experiments and modeling, Wear (2007), doi:10.1016/j.wear.2007.03.026

Table 2
Parameter values for CVFC model

	Pellet	Slider
Friction coefficient	$\mu_{dry,p} = 0.12$, unlubricated $\mu_p = 0.05$, good lubricant	$\mu_{dry,s} = 0.15$, unlubricated $\mu_s = 0.03$, good lubricant
Wear coefficient (m^2/N)	$K_p = 5.5 \times 10^{-8}$; $K_{ep} = 5.5 \times 10^{-9}$	$K_{es} = 5.5 \times 10^{-8}$
Normal load (N)	$F_p = 88.8$	$F_s = 0–225$

Disk values—sliding speed: $U = 27$ and 45 m/s; roughness: $h_{max} = 10^{-4}$ m.

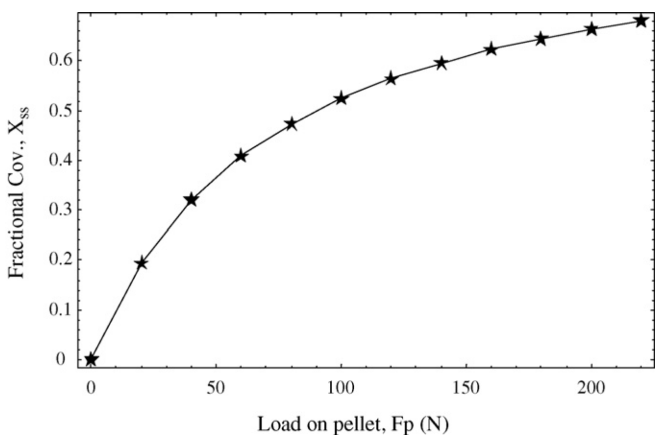

Fig. 8. Fractional coverage vs. pellet load.

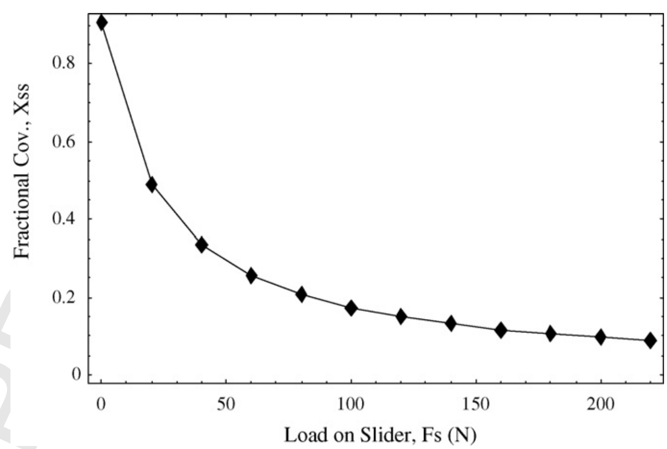

Fig. 9. Fractional coverage vs. slider load.

The results from Eqs. (8)–(10), and Eq. (13) form the basis for the comparison of the theoretical and experimental results in the next section.

4.2. Comparing experimental results with theory

The CVFC model qualitatively and quantitatively agrees with results from the pellet-on-disk with slider tests. In Figs. 8 and 9, the model predicted the fractional coverage parameter to increase with pellet load while decreasing with slider load, trends that were irrespective of the sliding velocity at steady state. Fig. 10a and b illustrate that at sliding speeds of 27 m/s and 45 m/s, both the model and experiment show the friction coefficient at the slider/disk interface increase before levelling off, as slider load increases. Finally, for the same sliding speeds of 27 m/s and 45 m/s, Fig. 11a and b shows that the theoretical and experimental wear factors for the pellet increase with slider load. This actually demonstrates that the pellet repairs the transfer film and self-replenishes the depleted film. Since the frictional response of powder lubricants are dependent on the environmental conditions, namely temperature and relative humidity, one should note that the CVFC model could be improved by including thermal variables in the model. This might certainly explain the deviations between experiments and theory at higher loads where the frictional heat increases.

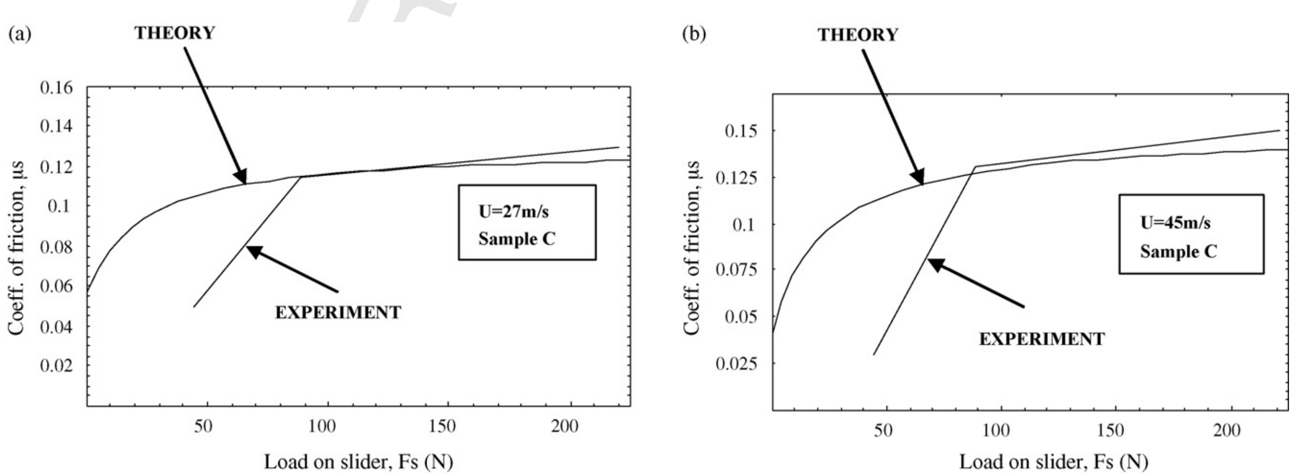

Fig. 10. Coefficient of friction vs. slider load.

Please cite this article in press as: C.F. Higgs III, E.Y.A. Wornyoh, An in situ mechanism for self-replenishing powder transfer films: Experiments and modeling, Wear (2007), doi:10.1016/j.wear.2007.03.026

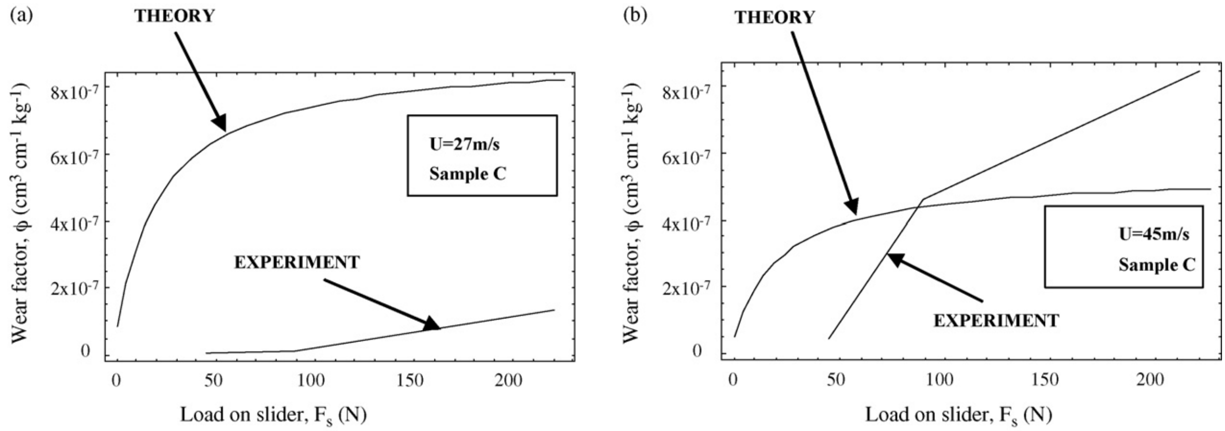

Fig. 11. Pellet wear factor vs. slider load.

5. Conclusion

Experiments were conducted to test the feasibility of developing a self-repairing, self-replenishing lubrication mechanism using powder lubrication. The results indicate that compacted MoS_2 in a competing-process tribosystem is a suitable candidate for providing continuous lubrication to sliding contacts. In order to predict the competing (deposition/depletion) lubrication process, a third-body control volume fractional coverage modeling approach was developed to predict slider friction and pellet wear on a pellet-on-disk with slider tribometer. The model is essentially based on first principle tribology with the only free parameters being the experimental wear coefficients. To that end, the model did an adequate job of predicting the friction coefficient at the slider/disk interface and the wear factor for the pellet. The experimental results also demonstrated that an in situ self-replenishing solid/powder lubrication mechanism could be developed using a pellet-on-disk with slider pad configuration.

Acknowledgements

The authors would like to thank Hooshang Heshmat, Ph.D. of Mohawk Innovative Technology Incorporated for developing the tribometer and introducing the authors to the powder lubrication mechanism. We would also like to thank the Pennsylvania Infrastructure Technology Alliance (PITA), the Philip & Marsha Dowd Foundation, and the Institute for Complex Engineering Systems at Carnegie Mellon University for supporting this work. The members of the Particle Flow & Tribology Laboratory (PFTL) engaged us in scholarly discussions on the model for which we are appreciative.

References

[1] C.F. Higgs III, H. Heshmat, Characterization of pelletized MoS_2 powder particle detachment process, J. Tribol. 123 (2001) 455–461.
[2] R. Kaur, H. Heshmat, 100 mm Diameter self-contained solid/powder lubricated auxiliary bearing operated at 30,000 rpm, Lubricat. Eng. 58 (6) (2003) 13–20.
[3] J.K. Lancaster, Lubrication by transferred films of solid lubricants, ASLE Trans. 8 (1965) 146–155.
[4] J.K. Lancaster, Anisotropy in the mechanical properties of lamellar solids and its effect on wear and transfer, Wear 9 (1966) 169–188.
[5] A.J. Haltner, An evaluation of the role of vapor lubrication mechanisms in MoS_2, Wear 7 (1964) 102–117.
[6] V. Johnson, G. Vaughn, Investigation of the mechanism of MoS_2 lubrication in vacuum, J. Appl. Phys. 27 (10) (1956) 1173.
[7] D.W. Dareing, S. Atluri, Traction behavior and physical properties of powder graphite lubricants compacted to Hertzian pressure levels, Tribol. Trans. 40 (3) (1997) 413–420.
[8] M. Godet, The 3rd-body approach—a mechanical view of wear, Wear 100 (1–3) (1984) 437–452.
[9] N. Fillot, I. Iordanoff, Y. Berthier, Simulation of wear through mass balance in a dry contact, J. Tribol. -Trans. ASME 127 (1) (2005) 230–237.
[10] S.D. Dvorak, K.J. Wahl, I.L. Singer, Friction behavior of boric acid and annealed boron carbide coatings studied by in situ Raman tribometry, Tribol. Trans. 45 (3) (2002) 354.
[11] M. Brendle, P. Turgis, S. Lamouri, A general approach to discontinuous transfer films: the respective role of mechanical and physicochemical interactions, Tribol. Trans. 39 (1) (1996) 157–165.
[12] W.G. Sawyer, T.A. Blanchet, Vapor-phase lubrication in combined rolling and sliding contacts: modeling and experimentation, J. Tribol. 123 (3) (2001) 572.
[13] P.L. Dickrell, et al., A gas-surface interaction model for spatial and time-dependent friction coefficient in reciprocating contacts: applications to near-frictionless carbon, J. Tribol. 127 (1) (2005) 82.
[14] W.G. Sawyer, P.L. Dickrell, A fractional coverage model for gas-surface interaction in reciprocating sliding contacts, Wear 256 (1/2) (2004) 73.
[15] P.L. Dickrell, W.G. Sawyer, A. Erdemir, Fractional coverage model for the adsorption and removal of gas species and application to superlow friction diamond-like carbon, J. Tribol. 126 (3) (2004) 615.
[16] E.Y.A. Wornyoh, C.F. Higgs III, Self-replenishing, Self-repairing solid lubrication: modeling and experimentation, in: Proceedings of the World Tribology Conference III, 2005.
[17] S. Jahanmir, M. Beltzer, An adsorption model for friction in boundary lubrication, ASLE Trans. 29 (3) (1986) 423–430.
[18] P.L. Dickrell, W.G. Sawyer, A. Erdemir, Fractional coverage model for the adsorption and removal of gas species and application to superlow friction diamond-like carbon, J. Tribol. -Trans. ASME 126 (3) (2004) 615–619.
[19] W.G. Sawyer, T.A. Blanchet, Vapor-phase lubrication in combined rolling and sliding contacts: modeling and experimentation, ASME J. Tribol. 123 (3) (2001) 572.